Development and Characterization of Au−YSZ Surface Plasmon Resonance Based Sensing Materials: High Temperature Detection of CO

George Sirinakis, Rezina Siddique, Ian Manning, Phillip H. Rogers, and Michael A. Carpenter*

College of Nanoscale Science and Engineering, The University at Albany—State University of New York, 255 Fuller Road, Albany, New York 12203

Received: May 5, 2006; In Final Form: May 9, 2006

Au−YSZ nanocomposite films exhibited a surface plasmon resonance absorption band around 600 nm that underwent a reversible blue shift and narrowed upon exposure to CO in air at 500 °C. A linear dependence of the sensing signal was observed for CO concentrations ranging between 0.1 and 1 vol % in an air carrier gas. This behavior of the SPR band, upon exposure to CO, was not observed when using nitrogen as the carrier gas, indicating an oxygen-dependent reaction mechanism. Additionally, the SPR band showed no measurable signal change upon exposure to CO at temperatures below ∼400 °C. The oxygen and temperature-dependent characteristics, coupled with the oxygen ion formation and conduction properties of the YSZ matrix, are indicative of charge-transfer reactions occurring at the three-phase boundary region between oxygen, Au, and YSZ, which result in charge transfer into the Au nanoparticles. These reactions are associated with the oxidation of CO and a corresponding reduction of the YSZ matrix. The chemical-reaction-induced charge injection into the Au nanoparticles results in the observed blue shift and narrowing of the SPR band.

Introduction

Growing environmental concerns associated with the use of fossil fuels have necessitated the development of gas sensors that can operate under harsh oxidizing or reducing environments in the temperature range between 500 and 900 °C. Although existing sensing technologies based on solid electrolytes, oxide semiconductors, and field effect devices exhibit significant potential for sensing applications at intermediate temperatures below 600 °C, there are major challenges associated with poor device stability and low selectivity that need to be addressed in order to expand their operational range to temperatures above 600 °C.[1−5] An alternative approach to gas sensing can be realized through optical methods such as absorption spectroscopy.[6] Optical sensing techniques are immune to electromagnetic noise and are inherently safer than their electrical counterpart, since the sensing elements are isolated from the interrogating electronics, thus minimizing the danger of explosion in environments with flammable or explosive gases.[7] Accordingly, significant experimental effort has been focused on the development of sensors that employ noble metal nanoparticles due to their unique optical properties. In particular, Au and Ag nanoparticles exhibit a strong surface plasmon resonance (SPR) band whose shape and spectral position is not only highly dependent on the refractive index of the host medium but also on chemical interactions, e.g., catalytic reactions at the interface between the metal and the surrounding environment.[8] Recently, Haruta and co-workers demonstrated the sensing potential of Au nanoparticles dispersed in a CuO matrix toward the detection of CO, at concentrations ranging from 50 to 10 000 ppm (1 vol %) in air at temperatures up to 300 °C.[9] The sensing mechanism was related to changes in the refractive index of the matrix due to the partial reduction of the CuO grains upon exposure to CO.

In the current work, the operational range of Au nanoparticle based sensing of CO was extended up to 500 °C through the use of a materials system comprised of Au nanoparticles embedded in a yttria-stabilized zirconia (YSZ) matrix. A reversible change in the optical properties of this nanocomposite is observed upon exposure to gas cycles of air and an air/CO mixture. The sensing mechanism has been attributed to high-temperature interfacial charge-transfer chemical reactions, occurring at the perimeter of the Au nanoparticles, which inject charge into the Au nanoparticle, causing changes in both the position and shape of the SPR band. These reactions are presumed to be associated with the reduction of the YSZ matrix and the oxidation of CO, via a charge-transfer reaction between YSZ-bound oxygen anions, formed through the dissociative adsorption of oxygen molecules on YSZ at high temperatures, and the Au nanoparticles.

Experimental Methods

The Au−YSZ nanocomposites were synthesized on sapphire substrates by rf magnetron co-sputtering followed by an annealing treatment at 1000 °C for 2 h. Films with a Au content of ∼10 at. % and a thickness of ∼30 nm were used for this study. The microstructure of the postannealed Au−YSZ films was examined by X-ray diffraction (XRD). The XRD pattern (see Supporting Information) indicated the presence of two polycrystalline phases, one corresponding to the tetragonal phase of YSZ and the other corresponding to the face-centered cubic Au phase. The average YSZ and Au crystallite sizes were calculated from the Scherrer formula[10] using the YSZ(101) and the Au(111) reflections, and an average crystallite size of ∼19 nm was obtained for both phases.

The sensing properties of the films at atmospheric pressure and elevated temperature were tested in a custom-designed quartz transmission cell housed within a tube furnace as shown schematically in Figure 1. White light from a CW Xe lamp was

* To whom correspondence should be addressed. Phone: (518) 437-8667. Fax: (518) 437-8603. E-mail: mcarpenter@uamail.albany.edu.

10.1021/jp062760n CCC: $33.50
Published on Web 06/17/2006

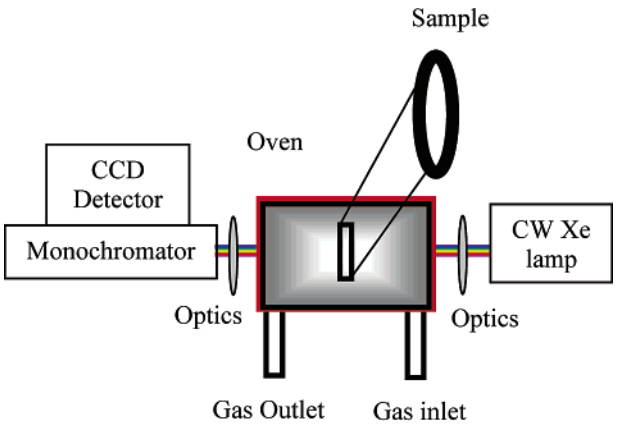

Figure 1. Schematic diagram outlining the high-temperature transmission cell testing bench assembly.

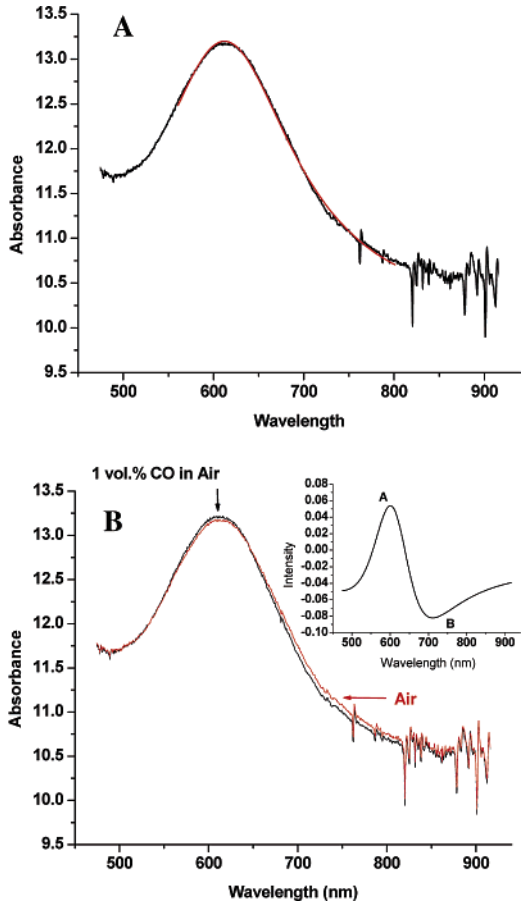

Figure 2. (A) Absorbance spectra of the Au−YSZ nanocomposite film in air at 500 °C with a corresponding Lorentzian curve fit. (B) Absorption spectra for air and 1 vol % CO in air at 500 °C. The inset graph displays the difference spectrum obtained by subtracting the fitted data resulting from the air and the air/CO exposures.

collimated and transmitted through the sample held centered in the quartz cell using a Macor sample holder. The transmitted light was dispersed and detected using a spectrometer equipped with a charged coupled diode (CCD) detection system. Air or air/CO (99.998% purity) gas exposures were delivered to the transmission cell via two mass flow controllers while a constant total flow of 2000 sccm at a pressure of 1 atm was maintained.

Results and Discussion

Figure 2A displays the absorption spectrum along with a corresponding Lorentzian fit to the data for a representative Au−YSZ film in the spectral region between 470 and 920 nm at 500 °C in an air background. Noise levels at the longer wavelength limit of the spectrum become rather pronounced due to the incomplete removal of the Xe lines from the absorption spectrum. The SPR band peaks at ∼600 nm and was fitted to a Lorentzian curve, with an R^2 value of 0.998, in the region between 560 and 800 nm, to extract the changes in the spectrum upon exposure to the air/CO mixture. This fitting range was dictated at the shorter wavelengths by the Au interband transitions, which have an onset at ∼520 nm, while wavelengths longer than 800 nm were ignored due to the pronounced noise levels. Figure 2B displays the absorption spectra of the Au−YSZ nanocomposite for both the air and an air/CO (1 vol %) gas mixture. In both cases a SPR absorption band at ∼600 nm was observed, however, upon exposure to CO the SPR band slightly blue shifts and becomes narrower, with no measurable change in the baseline of the spectrum at the short and long wavelength limits. The inset of Figure 2B displays the difference spectrum obtained by subtracting the fitted air and air/CO absorption spectra. The CO sensing signal is defined as the peak-to-peak difference between points A and B on the difference spectrum.

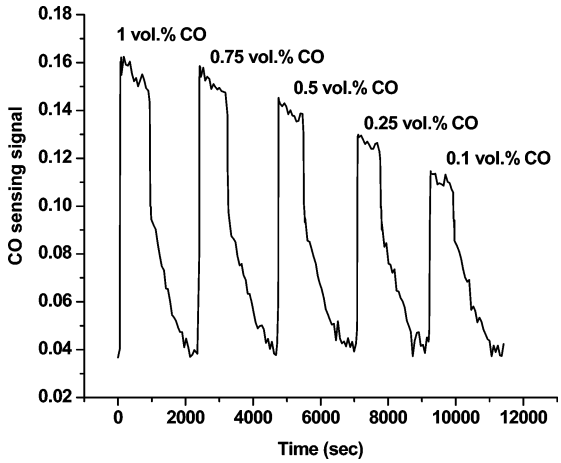

Figure 3. Sensing signal response curve of the Au−YSZ nanocomposite film upon exposure to 1, 0.75, 0.5, 0.25, and 0.1 vol % CO in air at 500 °C.

Figure 3 displays the resulting CO sensing signal as a function of time for the Au−YSZ film upon exposure to 1, 0.75, 0.5, 0.25, and 0.1 vol % CO concentrations in air at 500 °C. The change in the absorption spectra upon exposure to CO was reversible, and the sensing signal increased with increasing CO concentration. A background signal of ∼0.04 is observed during each of the air cycles and is attributed to the incomplete subtraction of the fitted spectra due to the noise levels observed in the raw data. The response time, i.e., the time required for the sensing signal to obtain its maximum value upon exposure to CO, was ∼40 s at all CO concentrations, with recovery in the subsequent air pulse displaying a two-stage mechanism comprised of a fast (∼60 s) initial stage followed by a slower (∼1000 s) stage.

Figure 4 reports the change in sensing signal, normalized to that observed for the 1 vol % CO exposures, plotted vs CO concentration at 500 °C. The data in Figure 4 were obtained from three individual runs and indicate a reproducible response toward CO. The increase in signal was nearly linear over a CO concentration range between 0.1 and 1 vol %. While this initial data set is promising for the potential development of an optical based method for the detection of CO under harsh operating conditions, a complete set of reliability tests will be required

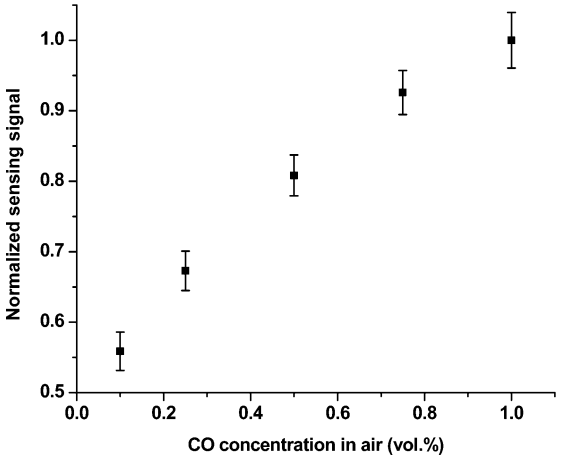

Figure 4. Normalized sensing signal vs CO concentration at 500 °C averaged over three separate exposure experiments. The signal at 1 vol % CO in air was normalized to be unity.

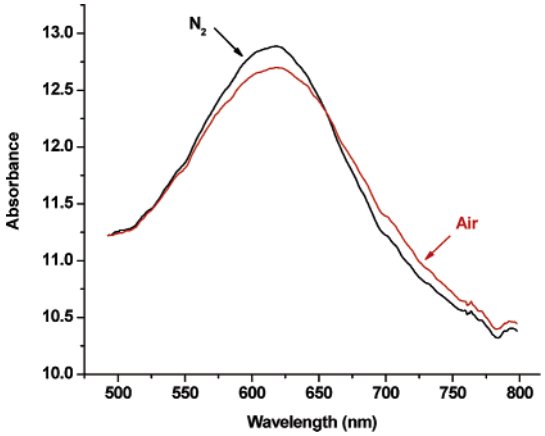

Figure 5. Absorbance spectra of Au−YSZ nanocomposite films in a N_2 and an air atmosphere at 500 °C.

and are underway to determine the long-term operating characteristics of this nanocomposite material.

Of particular interest for this system is an analysis of the optical properties of the YSZ-embedded Au nanoparticles as a function of the high-temperature reaction environment. The bulk of the literature on the sensing properties of noble metal nanoparticles reports on shifts of the SPR band, which within the context of Mie theory are attributed to changes in the refractive index of the local environment of the nanoparticle upon exposure to the target molecule.[9,11−13] However, apart from changes in the spectral position, changes in the width of the SPR band can also be used as a sensing signal and are indicative of a change in the chemistry at the nanoparticle interface. Specifically, the width of the SPR band depends on the damping of the collective motion of the conduction electrons and, therefore, will not only depend on material properties, which can be expressed via material parameters such as the dielectric functions of the nanoparticles and the surrounding matrix but also on the nature of the interface between the metal and the surrounding medium. In this respect, physisorption, chemisorption, or chemical interface reactions are expected to affect the width of the SPR band.[14] For the Au−YSZ system, we have previously performed detailed baseline optical and material analyses. These prior investigations observed a typical red shift of the SPR band with an increase in particle diameter and a rather weak interaction between the Au nanoparticles and the surrounding YSZ matrix at room temperature.[15,16] However, at elevated temperatures in the presence of oxygen, additional chemical reactions associated with the oxidation of YSZ are expected to take place at the perimeter of the Au nanoparticles and therefore affect the optical properties of the nanocomposite. Specifically, due to the increased amount of oxygen vacancies introduced in the zirconia matrix with the incorporation of yttrium, YSZ exhibits a high reactivity toward oxygen.[17] This well-documented reactivity is further enhanced by the presence of an electronic conductor such as Au, which provides a source of electrons at the three-phase boundary region between oxygen, Au, and the YSZ matrix and facilitates the formation of primarily ionized molecular or atomic oxygen species rather than their neutral counterparts.[18] Accordingly, in the specific case of the Au−YSZ nanocomposite, the removal of free electrons from the Au nanoparticle upon the dissociative adsorption and ionization of oxygen would manifest itself as a red shift and a broadening of the SPR band.[19−21] Figure 5 plots the absorbance spectra of Au−YSZ nanocomposites in a N_2 and in an air environment at 500 °C. A slight red shift and a broadening of the SPR band were observed upon switching from an oxygen-free N_2 atmosphere to air, consistent with the above discussion.

This finding when coupled with the experimentally observed reversible narrowing and slight blue shift of the SPR band upon exposure to CO suggests a change in both the chemical properties at the interface between the Au nanoparticle and the YSZ matrix and an increase in the free electron density of the Au nanoparticles. The high-temperature reactivity of CO with the Au−YSZ material system is further corroborated by the well-documented catalytic activity of Au nanoparticles toward CO oxidation, which is believed to increase significantly when the nanoparticle size is reduced below ∼4 nm.[22,23] Although the Au nanoparticle size used in this study is ∼19 nm, recent experimental work indicated that, for the Au−ZrO_2 system, the catalytic activity of Au nanoparticles can be improved when the size of the Au nanoparticle is comparable to the particle size of ZrO_2.[24] Likewise, in this work the XRD data along with the ∼30 nm thickness of the nanocomposite film indicate that the average particle size of the YSZ matrix is similar to the Au nanoparticle size. In this way, the number of contact boundaries between the Au nanoparticles and the adjacent matrix grains are maximized. This maximized contact area is believed to be crucial for the activation of oxygen in the CO oxidation reaction.[25] Therefore, for the Au−YSZ system it may be argued that at elevated temperatures, in the presence of oxygen, electrons are removed from the Au nanoparticle upon the dissociative adsorption and ionization of the oxygen species, thus creating a positively charged metal center in the immediate vicinity of the nanoparticle−matrix interface. Upon exposure to CO, ionized oxygen species are consumed by the CO oxidation reaction and electrons are transferred back to the positively charged Au nanoparticle. In this way the electron density is increased from the baseline conditions observed in an air background, thus resulting in a blue shift and narrowing of the SPR band.[26,27]

To provide a more complete understanding of the sensing mechanism, we have studied the behavior of the SPR band in the presence of 1 vol % CO in air as a function of temperature (25, 140, 320, 410, and 500 °C), as detailed in the sensing signal vs temperature graph shown in Figure 6. The Au SPR band shows no measurable signal change at 320 °C and below, while at 410 and 500 °C the characteristic blue shift and narrowing of the SPR band, similar to that shown in Figure 2, was observed. The onset of the resulting CO sensing signal change

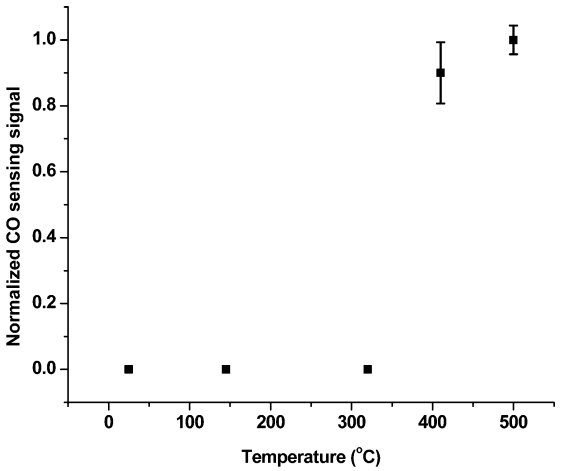

Figure 6. Normalized CO sensing signal vs temperature for 1 vol % CO in air gas exposures.

in Figure 6 coincides with the activation of oxygen ion transport within YSZ.[6]

To further elucidate the role of oxygen to the CO-sensing mechanism, CO exposures were performed in a dry N_2 environment. No measurable change in the SPR band was observed, thus confirming the essential role of O_2 in the sensing mechanism. This finding, when coupled with the blue shift and narrowing of the SPR band upon exposure to air and CO mixtures, suggests the presence of a charge-transfer-mediated catalytic chemical reaction at the interface of the Au nanoparticle and the YSZ matrix that enables the CO oxidation reaction.

Conclusions

Au−YSZ nanocomposite films were synthesized using the rf co-sputtering technique followed by an annealing treatment at 1000 °C. The nanocomposite films exhibited an SPR absorption band around 600 nm. Upon exposure to CO in ambient air at 500 °C the SPR band underwent a reversible blue shift and a narrowing of the fwhm. The change in the SPR band increased linearly with increasing CO concentration in the range between 0.1 and 1 vol %. Additionally, the presence of O_2 and sufficiently high temperatures for oxygen ion transport in YSZ were confirmed to be essential elements for the sensing mechanism. The behavior of the SPR band upon exposure to CO in the presence of air was attributed to changes both in the free electron density of the Au nanoparticles and in the interfacial chemistry due to reactions associated with the reduction of the YSZ matrix and oxidation of CO. This finding may have significant implications for the tailoring of nanocomposite films for optical sensing applications, as well as for developing an improved understanding of the nanoparticle optical property dependence on chemical processes taking place at the Au nanoparticle−matrix interface.

Acknowledgment. This work was supported by the United States Department of Energy National Energy Technology Laboratory, under contract number DE-FG26-04NT42184, and the New York State Office of Science, Technology and Academic Research (NYSTAR). Any opinions, findings, and conclusions or recommendations expressed in this publication are those of the authors and do not necessarily reflect the views of the United States Department of Energy National Energy Technology Laboratory. We also thank Prof. Richard Matyi for technical support with the XRD data.

Supporting Information Available: The X-ray diffraction spectrum of the Au−YSZ nanocomposite film collected using a Bruker D8 ADVANCE X-ray diffractometer in a standard $\theta-2\theta$ mode, with 2θ ranging from 25 to 55°. This material is available free of charge via the Internet at http://pubs.acs.org.

References and Notes

(1) Göpel, W.; Reinhardt, G.; Rösch, M. *Solid State Ionics* **2000**, *136*, 519.
(2) Fleischer, M.; Meixner, H. *J. Vac. Sci. Technol. A* **1999**, *174*, 1866.
(3) Park, C. O.; Akbar, S. A. *J. Mater. Sci.* **2003**, 38, 4611.
(4) Schalwig, J.; Müller, G.; Ambacher, O.; Stutzmann, M. *Phys. Stat. Sol. (a)* **2001**, *185*, 39.
(5) Spetz, A. L.; Baranzahi, A.; Tobias, P.; Lundstörm, I. *Phys. Stat. Sol. (a)* **1997**, *162*, 493.
(6) Docquier, N.; Candel, S. *Prog. Energy Combust. Sci.* **2002**, *28*, 107.
(7) Sbervegliery, G. *Gas Sensors*; Kluwer Academic Publishers: Norwell, MA, 1992.
(8) Kreibig, U.; Vollmer, M. *Optical Properties of Metal Clusters*; Springer: New York, 1995.
(9) Ando, M.; Kobayashi, T.; Iijima, S.; Haruta, M. *Sens. Actuators, B* **2003**, *96*, 589.
(10) Cullity, B. D.; Stock, S. R. *Elements of X-ray Diffraction*, 3rd ed.; Prentice-Hall: New York, 2001.
(11) Haes, A. J.; Van Duyne, R. P. *J. Am. Chem. Soc.* **2002**, *124*, 10596.
(12) MacFarland, A. D.; Van Duyne, R. P. *Nano Lett.* **2003**, *3*, 1057.
(13) Mock, J. J.; Smith, D. R.; Schultz, S. *Nano Lett.* **2003**, *3*, 485.
(14) Hövel, H.; Fritz, S.; Hilger, A.; Kreibig, U.; Vollmer, M. *Phys. Rev. B* **1993**, *48*, 18178.
(15) Sirinakis, G.; Siddique, R.; Monokroussos, C.; Carpenter M. A.; Kaloyeros A. E. *J. Mater. Res.* **2005**, *20*, 2516.
(16) Sirinakis, G.; Siddique, R.; Dunn, K. A.; Efstathiadis, H.; Carpenter, M. A.; Kaloyeros, A. E.; Sun, L. *J. Mater. Res* **2005**, *20*, 3320.
(17) Nowotny, J.; Bak, T.; Nowotny M. K.; Sorrell, C. C. *Adv. Appl. Ceram.* **2005**, *104*, 147.
(18) Nowotny, J.; Bak, T.; Nowotny M. K.; Sorrell, C. C. *Adv. Appl. Ceram.* **2005**, *104*, 154.
(19) Hosoya, Y.; Suga, T.; Yanagawa, T.; Kurokawa, Y. *J. Appl. Phys.* **1997**, *81*, 1475.
(20) Kreibig, V.; Genzel, L. *Surf. Sci.* **1985**, *156*, 678.
(21) Linnert, T.; Mulvaney, P.; Henglein, A. *J. Phys. Chem.* **1993**, *97*, 679.
(22) Haruta, M.; Daté, M. *Appl. Catal. A* **2001**, *222*, 427.
(23) Haruta, M. *Gold Bull.* **2004**, *37*, 27.
(24) Zhang, X.; Wang, H.; Xu, B. *J. Phys. Chem. B.* **2005**, *109*, 9678.
(25) Guzman, J.; Carrettin, S.; Fierro-Gonzalez, J.; Hao, Y.; Gates, B.; Corma, A. *Angew. Chem., Int. Ed.* **2005**, *44*, 4778.
(26) Hirakawa, T.; Kamat, P. V. *J. Am. Chem. Soc.* **2005**, *127*, 3928.
(27) Oldfield, G.; Ung, T.; Mulvaney, P. *Adv. Mater.* **2000**, *12*, 1519.